Atmos. Chem. Phys. Discuss., https://doi.org/10.5194/acp-2017-1161
Manuscript under review for journal Atmos. Chem. Phys.
Discussion started: 20 December 2017

Atmospheric Chemistry and Physics Discussions

Middle atmospheric ozone, nitrogen dioxide, and nitrogen trioxide in 2002–2011: SD-WACCM simulations compared to GOMOS observations

Erkki Kyrölä[1], Monika E. Andersson[1], Pekka T. Verronen[1], Marko Laine[1], Simo Tukiainen[1], and Daniel R. Marsh[2]

[1]Finnish Meteorological Institute, Earth Observation Unit, P.O. Box 503, 00101 Helsinki, Finland
[2]National Center for Atmospheric Research, Boulder, Colorado, USA

Correspondence to: Erkki Kyrölä (erkki.kyrola@fmi.fi)

Abstract. Most of our understanding of the atmosphere is based on observations and their comparison with model simulations. In the middle atmosphere studies it is common practice to use an approach, where the model dynamics is at least partly based on temperature and wind fields from an external meteorological model. In this work we test how closely satellite measurements of a few central trace gases agree with this kind of model simulation. We use collocated vertical profiles where each satellite measurement is compared to the closest model data.

We compare profiles and distributions of O_3, NO_2, and NO_3 from the Global Ozone Monitoring by Occultation of Stars instrument (GOMOS) on ENVISAT with simulations by the Whole Atmosphere Community Climate Model (WACCM). GOMOS measurements are from nighttime. Our comparisons show that in the stratosphere outside the polar regions differences in ozone between GOMOS and WACCM are small. The correlation of monthly and 5-day time series show very high correlation. In the tropical region in the lower stratosphere WACCM shows consistently larger values than GOMOS. In the polar areas GOMOS measurements show ozone losses that can be connected to the elevated NO_2 concentrations from solar storms and strong down draft events from the thermosphere that take place in the winter polar regions. In the mesosphere above the ozone minimum at 0.01 hPa (or 80 km) large differences are found between WACCM and GOMOS. Correlation can still be high, but at the second ozone peak correlation falls strongly and the ozone abundance from WACCM is about 60% smaller than from GOMOS. Outside the polar areas and in the validity region 25–0.3 hPa GOMOS and WACCM NO_2 agree reasonably well and the correlation is reasonably high except in the upper stratosphere in the southern latitudes. In the polar areas, where solar particle precipitation and downward transport from the thermosphere enhance NO_X abundance, large differences are found between GOMOS and WACCM NO_2. For NO_3, we find WACCM values agreeing largely with GOMOS with very high correlation. We show that NO_3 values depend very sensitively on temperature. The ratio of O_3 to NO_3 follows closely to the prediction from the equilibrium chemical theory. Abrupt temperature increases from Sudden Stratospheric Warmings are reflected as sudden enhancements of GOMOS and WACCM NO_3 values. NO_3 values can therefore be used as a proxy for major stratospheric warmings.

Atmos. Chem. Phys. Discuss., https://doi.org/10.5194/acp-2017-1161
Manuscript under review for journal Atmos. Chem. Phys.
Discussion started: 20 December 2017

Atmospheric Chemistry and Physics Discussions

1 Introduction

The quality of atmospheric modelling is crucial for making reliable predictions for future climate. The minimum quality requirement for any model is that already measured central atmospheric variables can be simulated within reasonable accuracy. The increasing number of global satellite missions since the discovery of the ozone hole offers a good opportunity to compare models with observed data. Moreover, there is now improving understanding of the accuracy of satellite measurements (see e.g. Hubert et al., 2016; Hegglin and Tegtmeier, 2017; Tegtmeier et al., 2013) and this is an essential ingredient for a model-measurement comparison.

In this work, we make use of the Whole Atmosphere Community Climate Model (WACCM) from the National Center for Atmospheric Research and compare its results to satellite observations from the Global Ozone Monitoring by Occultation of Stars instrument (GOMOS). We concentrate on an atmospheric region ranging from the stratosphere to lower thermosphere (20–100 km) and on three important minor constituents O_3, NO_2, and NO_3 measured by GOMOS.

Ozone is a central chemical element in the middle atmosphere and essential for stopping short wave UV-light from entering into the biosphere. Ozone has diurnal variability, which in the stratosphere is weak, but at 90–95 km nighttime ozone can be an order of magnitude more abundant that during daytime (see e.g. Kyrölä et al. (2010a)). Measured satellite ozone profiles are validated using ozone sondes and ozone lidars. Comparisons to other satellite measurements also help to establish the data quality. Nitrogen dioxide, as a member of the odd nitrogen family, participates in catalytic destruction of ozone especially in the upper stratosphere (Lary, 1997). In polar areas precipitation of charged particles creates vast amount of NO_x which has a long chemical lifetime in the polar darkness. When isolated by a stable vortex, enhanced NO_x can descend into the upper stratosphere, which then leads to natural ozone loss when NO_x becomes illuminated by increasing solar light after the winter season (e.g. Seppälä et al., 2007; Päivärinta et al., 2016). Polar NO_x is also enhanced by polar descent from the thermosphere and exceptionally large increases have measured after so-called Sudden Stratospheric Warming events (SSW) where the vortex structure is disturbed (see Hauchecorne et al., 2007; Randall et al., 2009; Smith et al., 2009; Sofieva et al., 2012; Chandran and Collins, 2014). Nitrogen trioxide is a part of the O_3-NO_2-NO chemistry. Nitrogen trioxide has a very strong diurnal variation and it is almost absent during daytime.

WACCM is the atmospheric component of the Community Earth System Model (CESM) (Neale et al., 2013). WACCM is a chemistry - climate model spanning the range of altitude from Earth's surface to the thermosphere (approximately 140 km) with 88 vertical levels of variable vertical resolution of 1.1 km in the troposphere to 3.5 km above 65 km (Marsh et al., 2013). Horizontal resolution is 1.9 deg. latitude by 2.5 deg. longitude and the model time step is 30 minutes. In the present analysis version 4 of WACCM was run in specified dynamics mode by constraining dynamical fields to Modern-Era Retrospective Analysis for Research and Applications (MERRA) meteorological re-analyses below 1 hPa. Above the stratopause WACCM dynamics are solved in a free running mode, i.e. temperature and dynamic fields are self-determined (although in practice they are still strongly modulated by MERRA). The version of WACCM used in this work includes chemistry of the lower, D-region ionosphere (see Verronen et al., 2016).

Atmos. Chem. Phys. Discuss., https://doi.org/10.5194/acp-2017-1161
Manuscript under review for journal Atmos. Chem. Phys.
Discussion started: 20 December 2017

Atmospheric Chemistry and Physics Discussions

WACCM has been evaluated in many model-measurement intercomparison studies. In Eyring et al. (2013), WACCM's total ozone values and trends were shown to be in reasonable agreement with satellite observations. Results showed that WACCM compares well with HALOE's stratospheric ozone measurements. Comparisons at specific atmospheric conditions have provided more information on the agreement between WACCM and observations. In Tweedy et al. (2013), the simulated behaviour of the secondary ozone maximum is compared against SABER measurements during a major sudden warming. The behaviour during SSWs was found to be similar while the nighttime ozone amount is generally underestimated by about a factor of two in WACCM. Comparisons of NO_x during polar winter, when NO_x is influenced by energetic particle precipitation, have been made in many studies (Jackman et al., 2011; Funke et al., 2011; Randall et al., 2015; Andersson et al., 2016; Funke et al., 2017). From these studies it seems that WACCM tends to underestimate mesospheric NO_x by a factor of $\sim$4.

GOMOS (Bertaux et al., 2010) was an instrument on the European Space Agency's ENVISAT satellite which was in operation for just over ten years between 2002 and 2012. The measurement method of GOMOS, stellar occultation, uses light from 180 brightest stars allowing global coverage of measurements with good vertical resolution. The occultation method is self-calibrating because the occulted star's spectrum is also measured without the atmospheric intervention and therefore the primary source data for retrievals (i.e., transmissions) are in principle stable. GOMOS measured 880,000 stellar occultations during the lifetime of ENVISAT. Ozone's relatively large abundance makes it quite an easily observable constituent from satellite instruments using optical measurements. GOMOS measurements can be used to retrieve ozone at altitudes ranging from the troposphere to the mesosphere and lower thermosphere. NO_2 and NO_3 can be retrieved in the stratosphere.

Our comparison of GOMOS measurements with WACCM simulations will be based on comparison of individual, co-located profile measurements, whereas in many other model-data studies climatological or other average quantities are used. Our method avoids the problem of uneven (in geolocation and time) sampling that accompanies limb and especially limb occultation measurements and distorts climatologies. In the Coupled Model Intercomparison Project (CMIP) and in the more specialised Chemistry-Climate Model Initiative (CCMI) several atmospheric (or more generally earth system) models including CESM/WACCM have been compared with each other and also with observations (see Tilmes et al., 2016; Morgenstern et al., 2017; Eyring et al., 2010, 2013). Most of the interest in these studies is targeted on future climate projections especially in the troposphere. In this work we are interested to see how well a model simulates the whole middle atmosphere from the upper troposphere up to the lower thermosphere in a limited time range 2002–2011.

Our study is structured as follows. In Sec. 2 we introduce the GOMOS instrument and the measurements we are using in this work. In Sec. the main properties of the WACCM model are introduced. The comparison method is introduced in Sec. 4 and individual comparisons of O_3, NO_2 and NO_3 are presented in Secs. 5–7.

2 GOMOS measurements

GOMOS was a stellar occultation instrument on board ENVISAT that was operational from 2002 to 2012 (for GOMOS overviews, see Bertaux et al. (2010); ESA (2001), and https://earth.esa.int/web/guest/missions/esa-operational-eo-missions/envisat/instruments/gomos). GOMOS measured occultations during both day and night, but measurements during daytime

suffer from scattered solar light that had to be estimated and removed in order to isolate the stellar signal. So far this has approach not led to satisfactory results. In this work we use only GOMOS nighttime measurements.

GOMOS nighttime profiles of O_3, NO_2 and NO_3 are retrieved from the spectral range 248–690 nm. The integration time of the measurements is 0.5 s, which provides an altitude sampling resolution of 0.2–1.6 km depending on the tangent altitude and the azimuth angle of the measurement. The retrieved ozone profiles have a 2 km vertical resolution below 30 km and a 3 km resolution above 40 km, whereas NO_2 and NO_3 have a 3 km vertical resolution at all altitudes. Details of the GOMOS retrieval algorithms and data quality are discussed in detail in Kyrölä et al. (2010b) and Tamminen et al. (2010). In this work we use GOMOS data from the ESA processing version 6 in a vertically gridded form (for data access, see Sec. 10). We remove those data points that have been measured when ENVISAT was located in the region of the South Atlantic Anomaly. The illumination conditions for the GOMOS measurements are determined by two solar zenith angles controlling solar light at the tangent point and at the satellite location. At the tangent point we require that the zenith angle is greater than 104°. It has been shown that for zenith angles smaller than 118° at the satellite position some stray light can be present, but we have not found any discernible change in our results ignoring this restriction altogether. In the GOMOS gridded ozone data there are a special flag that labels stars that do not provide sufficient signal-to-noise ratio for reliable ozone retrieval in the mesosphere-lower thermosphere (faint and cool stars). Profiles considered as outlier either in the stratopshre or in the mesosphere are also flagged. We set all three flags equal to zero for ozone comparisons. The total number of GOMOS nighttime measurements is then 238 664. For NO_2 and NO_3 the ozone flags can be ignored and we get 377 881 measurements. The number of measurements peaked in 2004 and declined thereafter due to the problems connected to the steering mechanism of the instrument. During 2005 no measurements were collected from the period of from February to May due to this steering problem. Note that the polar regions are not covered by nighttime measurements during summer months. For other latitudes measurements cover all seasons.

The first comprehensive validation of GOMOS nighttime stratospheric ozone (ESA data version 4) against ground-based and balloon-borne instruments was presented in Meijer et al. (2004). The results showed that GOMOS nighttime ozone agrees within a few percent with the correlative data (sondes and lidars) in the stratosphere outside polar areas. An update of this work was issued by van Gijsel et al. (2010) using the ESA software version 5 and results were similar to Meijer et al. (2004). In this work we are using the ESA software version 6. All three versions (4–6) provide very similar results. The version 6 has been under validation in the ESA projects Valid-2 and Multi-TASTE and the validation reports are available from https://earth.esa.int/web/sppa/mission-performance/esa-missions/envisat/gomos/cal-val/validation-activities. Recent similar validation results can be found from Hubert et al. (2016) and Sofieva et al. (2016). Results show differences to be $\pm 3\%$ between 20–45 km. Below 20 km GOMOS show increasing positive bias in the tropics, but in this work we restrict analysis to higher altitudes where such bias is not observed. GOMOS and so-called gold standard of satellite ozone profiles, SAGE II, were compared in Kyrölä et al. (2013) and differences $\pm 4\%$ in 23–55 km were observed when the SAGE II sunrise and sunset occultations were treated separately. The diurnal variation of ozone in the stratosphere and some sunset-sunrise instrumental factors are contributing to these numbers (see also Sakazaki et al. (2015)). Climatological comparisons of several limb viewing satellite instruments including GOMOS are presented in Tegtmeier et al. (2013).

Atmos. Chem. Phys. Discuss., https://doi.org/10.5194/acp-2017-1161
Manuscript under review for journal Atmos. Chem. Phys.
Discussion started: 20 December 2017

Atmospheric Chemistry and Physics Discussions

GOMOS is able to measure ozone up to 100 km when stars with sufficiently high effective temperature are used. For mesospheric heights there are no real validation results, but we can get some insight from comparisons to other satellite measurements. In Verronen et al. (2005) GOMOS and MIPAS ozone were found to agree within $\pm 10\%$ in 25–70 km. Similar results were obtained in Ceccherini et al. (2008). SABER and GOMOS were compared in Smith et al. (2008, 2013), which showed that GOMOS mesospheric ozone values are about 20% smaller than SABER.

GOMOS measurements can nominally be used to retrieve NO_2 at altitudes between 25 and 50 km, while in the polar regions altitudes up to about 70 km can be reached during winter months due to higher NO_2 concentrations. There is only one publication where GOMOS NO_2 measurements have been compared with in-situ measurements. It is the comparison with balloon-borne instruments (Renard et al., 2008), which indicated an agreement within $\pm 25\%$. In addition, several comparisons against satellite-based observations have been made. Verronen et al. (2009) found that GOMOS NO_2 values are 10–25% higher than MIPAS. Comparison with ACE-FTS in Kerzenmacher et al. (2008) showed better than 10% agreement between 23 and 42 km. At higher altitudes larger differences were found, but the necessary correction for diurnal variation made results very uncertain. Nitrogen dioxide has a strong diurnal variation with maximum and minimum amounts seen during early night and early morning, respectively (for diurnal cycle from model simulations, see e.g., Brasseur and Solomon (2005); Kyrölä et al. (2010a). Climatological comparison with HALOE can be found in Hauchecorne et al. (2005).

GOMOS retrieval of NO_3 covers the altitude range 25–50 km. During daytime NO_3 almost vanishes by photolysis but rises quickly after the sunset from the reactions between O_3 and NO_2 (for diurnal cycle from model simulations, see e.g. Brasseur and Solomon (2005); Kyrölä et al. (2010a)). There are only few NO_3 measurements to which to compare GOMOS measurements. GOMOS NO_3 have been compared with two balloon measurements in Renard et al. (2008), but with inconclusive results. In Hakkarainen et al. (2012) GOMOS measurements were compared with SAGE III lunar measurements and the agreement was found to be within $\pm$ 25%.

3 SD-WACCM-D simulations

WACCM includes the O_x, NO_x, Cl_x and BrO families and CH_4 with its reaction products. The number of reactions is 217 with 59 species. Heterogeneous reactions with three types of aerosols are also included. The model includes orographic and nonorographic gravity waves (see Garcia et al., 2007). The upper boundary temperature condition is given by the MSIS-model by Hedin (1991). The same model is used to specify O, O_2, H and N upper boundary conditions. At the lower boundary observations are used to specify the surface mixing ratios of CFC-gases, CH_3, N_2O and other important gases for stratospheric processes. The solar irradiance is provided by the model of Lean et al. (2005) which takes into account the spectral and flux variations during the solar cycle. WACCM includes ionisation rates from Solar Proton Events (SPE) and auroral electrons. More details of the WACCM model can be found from Marsh et al. (2013), Smith et al. (2011), and Garcia et al. (2007).

In this work we use SD-WACCM-D version 4, i.e., the model a) includes chemistry of the lower, D-region ionosphere required for detailed EPP simulations (see Verronen et al., 2016) and b) is run in specified dynamics (SD) mode by constraining dynamical fields below 1 hPa to Modern-Era Retrospective Analysis for Research and Applications (MERRA) meteorological

Atmos. Chem. Phys. Discuss., https://doi.org/10.5194/acp-2017-1161
Manuscript under review for journal Atmos. Chem. Phys.
Discussion started: 20 December 2017

re-analyses (see Rienecker et al., 2011). SD mode allows for realistic representation of atmospheric dynamics making the simulations directly comparable to satellite observations, while the D-region ion chemistry has been shown to improve the polar mesospheric comparisons for many species, including NO_x (Andersson et al., 2016). In order to provide an ion source for the low-latitude D-region chemistry, ionisation due to galactic cosmic radiation is included in our simulations using the Nowcast of Atmospheric Ionising Radiation for Aviation Safety (NAIRAS) model (for details, see Jackman et al., 2016). For this study, we also include the ionisation due to 30–1000 keV radiation belt electron precipitation in the energetic particle forcing. For details on the precipitation model and ionisation rate calculation, see van de Kamp et al. (2016). In this energy range, electrons add to HO_x and NO_x production in-situ at 60–90 km altitude, directly affecting mesospheric ozone chemistry at geomagnetic latitudes between 55° and 72° (Matthes et al., 2016). The ionisation rates are applied in WACCM as daily, zonal mean values which depend on the geomagnetic A_p index and latitude.

4 Comparison method

In order to compare GOMOS vertical profiles with WACCM simulations each satellite measurement is paired with the closest WACCM latitude-longitude-time profile (i.e., no interpolation between different WACCM grid cells is done). The geolocation of the satellite measurement is defined by the average value when the line-of-sight of the instrument is between the altitudes 20–50 km. In this study, we compare all GOMOS nighttime measurements from 2002 to 2011 to a WACCM simulation run for the same period. For the satellite measurements the comparison is complete in the sense that every measurement finds its model partner with a very good co-location limits: latitude difference smaller than 0.95 deg., longitude difference smaller than 1.25 deg, and time difference shorter than 15 min. This method avoids the problem of uneven (in geolocation and time) sampling that accompanies limb and especially limb occultation measurements and which may distort trace gas climatologies and their comparisons.

A retrieved GOMOS constituent profile is given at the measurement's refracted line-of-sight altitudes that vary from one measurement to another. In this work we interpolate (linearly) the profiles to a regular geometric altitude grid with one km step. GOMOS constituent abundances are given in number densities. WACCM runs on a pressure grid and abundances are mixing ratios. In order to compare satellite measurements with WACCM we need either to change satellite measurements to the pressure grid of WACCM or to change WACCM results to the altitude grid used by satellite data. We have selected to work using the WACCM's pressure grid. Therefore, every GOMOS measurement is interpolated to the altitudes obtained from the geopotential heights of the WACCM's latitude-longitude cell nearest to the satellite measurement at the time of the measurement. This brings the number densities of satellites to the pressure grid of the model. In this work we show results in mixing ratios as they more suitable for illustrating results. The transformation to mixing ratios is accomplished by the neutral density distribution of WACCM (coming in the SD-version from MERRA and internal dynamics).

The method we use for comparing collocated satellite and WACCM profiles and their differences at each altitude z is to calculate the bias over a suitable number of profiles in a selected region (time and geolocation) as

$$B(z) = \langle f_{\mathrm{k}}^{\mathrm{W}}(z) - f_{\mathrm{k}}^{\mathrm{G}}(z) \rangle, \quad (1)$$

Atmos. Chem. Phys. Discuss., https://doi.org/10.5194/acp-2017-1161
Manuscript under review for journal Atmos. Chem. Phys.
Discussion started: 20 December 2017

Atmospheric Chemistry and Physics Discussions

where $f_{\mathrm{k}}^{\mathrm{W}}$ denotes WACCM and $f_{\mathrm{k}}^{\mathrm{G}}$ GOMOS collocated vertical profiles. Satellite gridded profiles have some missing data from flagged data points or from restrictions of the altitude coverage of measurements. The corresponding WACCM data points are ignored in the average in order to preserve the complete correspondence of the data sets. For practical reasons we will also use the bias in a relative sense as

$$\Delta(z) = 100\frac{B(z)}{\langle f_{\mathrm{k}}^{\mathrm{G}}(z)\rangle}. \quad (2)$$

The scaling factor (denominator) is calculated from WACCM in the same region as the bias.

Calculation of the average estimates is based on dividing spatial and temporal extensions to suitable scales. We average data within 10 degrees in latitude and use zonal averaging. For the polar regions we also show results from a larger latitudinal range (from 60 to 90 degrees south and north). In the time domain the analysis is based on monthly averages, but for the polar regions we use 5-day time series in order to capture fast polar processes keeping still reasonable statistical accuracy. From the time series we calculate the WACCM-GOMOS mission average biases and correlation coefficients $C(z)$.

The formula Eq. (1) includes averages over number of GOMOS-WACCM data pairs. In this work we extend the average over all quality filtered data 2002–2011. Before averaging clear outliers in data are removed by $|x - \mathrm{median}(x)| > 3 \times 1.4826 \times \mathrm{median}(|x - \mathrm{median}(x)|)$. Averages are calculated using the median estimator. The uncertainty is calculated by the error of the median (see e.g., Eq. (1) in Kyrölä et al. (2010a)).

For GOMOS knowing the validity limits of retrieved data is especially important as all 180 target stars have their own valid altitude ranges and outside the ranges results are often contaminated by noise. The GOMOS data we are using include star specific valid altitude limits for all three gases of this work. These limits are based on yearly averages. In order to handle rapidly changing events we need more dynamic determination of the validity ranges. Therefore, we calculate for each gas, latitudinal zone and time series period the t-value profile (the median value divided by its uncertainty) for each star included in the domain inspected. For the final average (over different stars) we include only those portions from the individual profiles where $t > 2$. The accepted $t > 2$ altitudes may form several separate altitude regions and some of them may not represent reliably the atmospheric state. In order to eradicate noise generated $t > 2$ regions, we accept only two largest continuous regions, both exceeding a prescribed minimum size. Two regions are needed in order to handle ozone profiles extending from lower stratosphere to the lower thermosphere. In the ozone minimum region around 0.01 hPa (80 km) density values are so small that $t > 2$ condition is not usually achieved but t-values recover again at higher altitudes. A similar case can be found with polar NO_2 profiles during solar storms where large increases of NO_2 take place above the normal validity range of NO_2.

The t-value method has at least one weakness and it is connected to the different behaviour of GOMOS retrievals and WACCM simulations at the situations where the density of a retrieved gas approaches to zero. When the density decreases the WACCM statistical distribution (from an averaging domain) changes from the approximate normal distribution (natural variation) to a nearly lognormal-type of distribution because of the physical lower limit zero in the model. The GOMOS retrieval method does not limit the retrieved gas values by a positivity condition as this could be a source of bias. As the density approaches to zero the GOMOS distribution remains usually nearly normal covering also negative values. Ideally this distribution would settle down around zero with the width given by the noise of the instrument. Unfortunately sometimes this

Atmos. Chem. Phys. Discuss., https://doi.org/10.5194/acp-2017-1161
Manuscript under review for journal Atmos. Chem. Phys.
Discussion started: 20 December 2017

Atmospheric Chemistry and Physics Discussions

does not happen and we see high altitude values with $t > 2$. These "ghost" detections may be generated by the interference of the other gases retrieved at the same time. At the moment we do not have any data based method to identify these ghost values. As a precautionary measure we reject those altitudes where the GOMOS distribution (from a given star, region, time, altitude) includes more than 20% negative values. For polar latitudes we apply a more relaxed limit of one-third, which allows the analysis to capture fast developing processes.

The final average form the averaging region and period of time is done by first making averages for each star and then averaging over all stars involved. This provides more equal contribution from different latitudes covered and no star can dominate the average by its high number of measurements.

5 Ozone

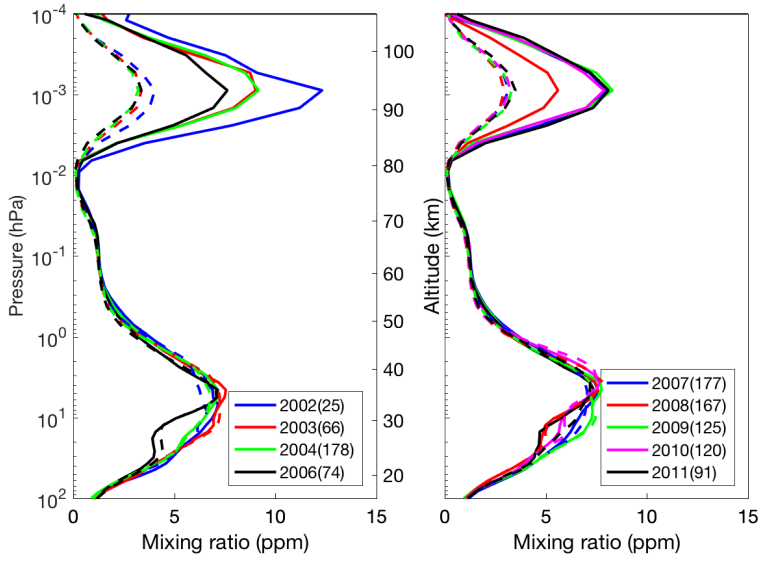

Figure 1. Ozone yearly median profiles from GOMOS Sirius occultations (solid lines) and from paired WACCM profiles (dashed lines) from 2002 to 2011 in the latitude band 40°S–60°S. The vertical axis is pressure. The approximate geometrical altitude is also shown. The colour coding in the legend boxes shows the measurement year and in the parenthesis the number of measurements.

As an example of retrieved satellite ozone profiles and paired WACCM profiles, we show in Fig. 1 observations from the brightest star in the sky, Sirius. It provides the best signal-to-noise ratio at all wavelengths of GOMOS stellar occultations. These measurements were taking place every year from the late August to mid-September In Fig. 1 we show the yearly median profiles from both the GOMOS observations and the WACCM simulation. It is evident that the observations and the model simulations generally agree well at all altitudes except in the neighbourhood of the second ozone peak (at 0.001 hPa, 91 km) where large differences and yearly variations are evident. The mission average 2002–2011 relative uncertainty of the GOMOS and WACCM Sirius profiles is better than 2% in the altitude range 100-0.05 hPa. The relative uncertainty grows to 10% at

Atmos. Chem. Phys. Discuss., https://doi.org/10.5194/acp-2017-1161
Manuscript under review for journal Atmos. Chem. Phys.
Discussion started: 20 December 2017

Atmospheric Chemistry and Physics Discussions

and around the ozone minimum at 0.01 hPa, but it reaches again 2% at the second peak and diverges at altitudes above. The WACCM-GOMOS relative difference stays inside $\pm 10\%$ between 50-0.05 hPa, but increases up to 60% at the second peak and grows still at higher altitudes. Differences are statistically sound in the mesosphere whereas in the lower atmosphere the differences fluctuate on both sides of zero.

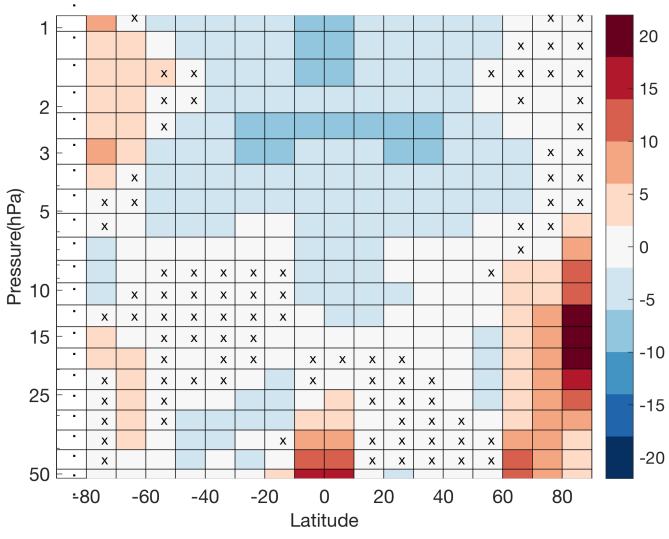

Figure 2. The median relative difference (WACCM-GOMOS)/median(GOMOS) of the ozone mixing ratio (in %) in the stratosphere over 2002–2011. Latitudes are from –90° to +90° with 10° resolution. A crossed cell marks a point where the difference does not deviate from zero in a statistical significant way. A cell with a dot marks missing data.

In order to get a more comprehensive view of WACCM-GOMOS differences for all latitudes we consider now ozone profiles from all eligible GOMOS occulted stars. Profiles flagged by the ozone flags are not included, but all others are included by those pressure levels that pass the t-value and the distribution criteria discussed earlier in Sec. 4. The altitude-latitude relative difference distribution between GOMOS and WACCM as a median average of 5-day (polar) and monthly (non-polar) time series from 2002 to 2011 is shown in Fig. 2 for the stratosphere and in Fig. 3 for the mesosphere-lower thermosphere. The validity range that applies to all latitudes is from 0.00012 hPa to 85 hPa. In both figures the differences are mostly statistically significant, points where the WACCM-GOMOS difference is insignificant are marked by crosses. In the stratosphere outside the polar latitudes differences are generally small, WACCM values being 0–6 % smaller than GOMOS. Both GOMOS and WACCM main ozone maxima are at the Equator at 10.3 hPa and the values agree within 2.5%. In the tropics in the lower stratosphere we see that WACCM values are larger (up to 20%) than GOMOS. This ozone surplus is found every year, but its seasonal strength varies. Notice that the tropical positive bias region of GOMOS discussed earlier in Sec. 2 resides below this region (not covered by the figure). In the polar regions GOMOS and WACCM agree within -2%–+6% except around 15 hPa

Atmos. Chem. Phys. Discuss., https://doi.org/10.5194/acp-2017-1161
Manuscript under review for journal Atmos. Chem. Phys.
Discussion started: 20 December 2017

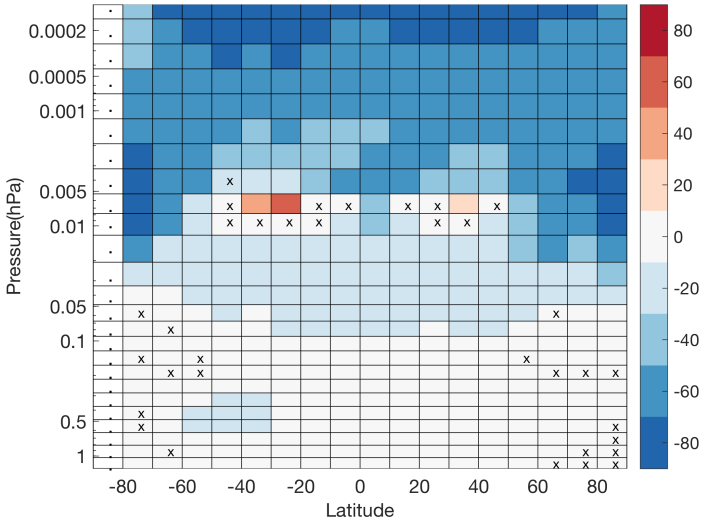

Figure 3. The median relative difference (WACCM-GOMOS)/median(GOMOS) of the ozone mixing ratio (in %) in the mesosphere over 2002–2011. Latitudes are from –90° to +90° with 10° resolution. A crossed cell marks a point where the difference does not deviate from zero in a statistical significant way. A cell with a dot marks missing data.

in 60°N–90°N where WACCM is up to 20% larger than GOMOS. Overall we can say that in the stratosphere GOMOS and WACCM agree nearly within the uncertainty estimates from GOMOS validation except in two cases mentioned.

Figure 3 shows the mesospheric differences, which are moderate up to the altitude 0.05 hPa or even up to the altitude 0.005 hPa outside the polar latitudes. Around 0.1 hPa in the polar areas GOMOS and WACCM agree within $\pm 5\%$. During wintertime a so-called tertiary ozone peak appears in this region (see e.g. Marsh et al., 2001; Sofieva et al., 2009). In the upper mesosphere differences grow strongly and WACCM values are about 60% smaller than GOMOS around the second ozone peak. A similar model-measurement difference has been seen in a Hammonia model study (see Schmidt et al. (2006)). Maximum mixing values are seen at the Equator where GOMOS mixing ratio is 10.5 ppm at 0.0005 hPa (96 km) and WACCM 4 ppm at 0.001 hPa (91 km) (Notice that WACCM's coarse pressure grid makes these estimates uncertain). In the studies of Tweedy et al. (2013); Smith et al. (2014) the difference was found to be around 70%. The ozone minimum is located at 0.009–0.015 hPa with minimum values above 0.1 ppm. Notice that GOMOS data uncertainty is large at the minimum and the relative difference varies from positive to negative. Overall we can say that in the mesosphere there is clear difference between GOMOS and WACCM. This result is in agreement between earlier comparisons. The GOMOS retrieval is very straightforward in the mesosphere and it is difficult to see how it could be in error by this large amount.

The ten year mission averaged bias is, of course, a narrow measure on the compatibility of GOMOS and WACCM. We now investigate how GOMOS and WACCM ozone values develop in time. Fig. 4 shows the correlation coefficient of GOMOS and WACCM from monthly (non-polar) and 5-day (polar) time series as a function of the altitude and latitude. In the stratosphere

Atmos. Chem. Phys. Discuss., https://doi.org/10.5194/acp-2017-1161
Manuscript under review for journal Atmos. Chem. Phys.
Discussion started: 20 December 2017

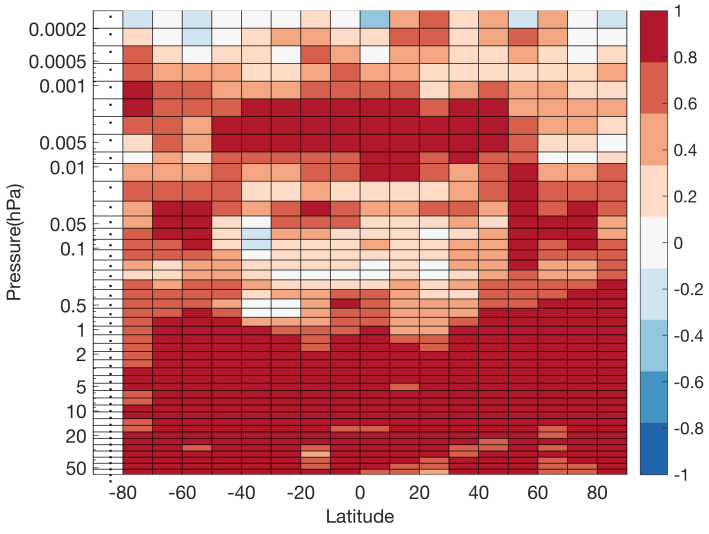

Figure 4. WACCM and GOMOS ozone mixing ratio correlation over 2002–2011. In the polar areas it is calculated from 5-day time series, in other latitudes it is calculated from monthly time series. Latitudes are from -90° to 90° with 10° resolution. A cell with a dot marks missing data.

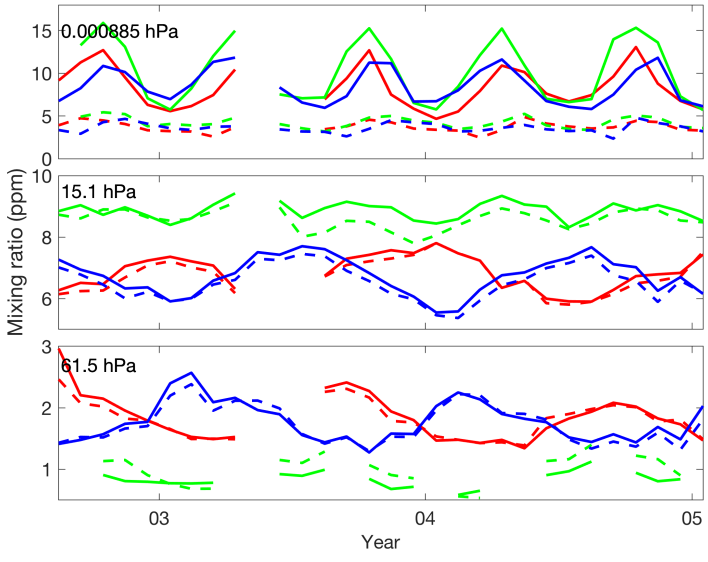

Figure 5. WACCM and GOMOS ozone monthly time series 1.8.2002–31.1.2005. Three latitude belts are shown: 50°S–30°S (red lines), 10°S–10°N (green) and 30°N–50°N (blue).

Atmos. Chem. Phys. Discuss., https://doi.org/10.5194/acp-2017-1161
Manuscript under review for journal Atmos. Chem. Phys.
Discussion started: 20 December 2017

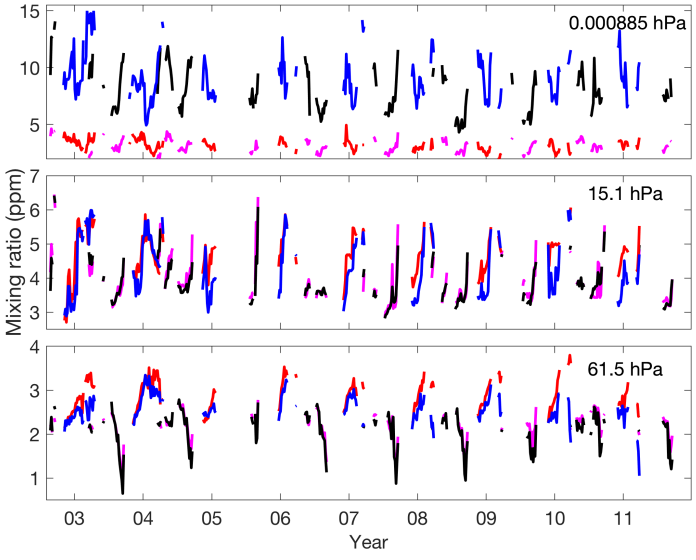

Figure 6. WACCM and GOMOS ozone mixing ratio 5-day time series from 2002–2011 in the Arctic 60°N–90°N (GOMOS: blue, WACCM: red) and in the Antarctic 60°S–90°S (GOMOS: black, WACCM: magenta).

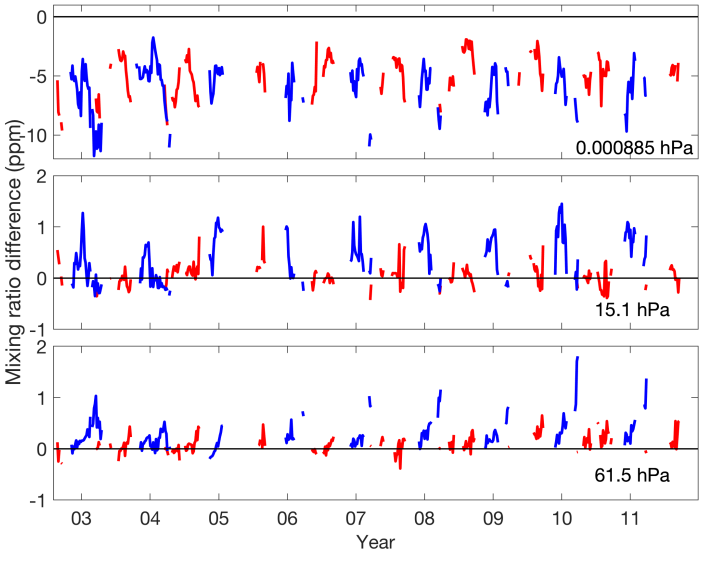

Figure 7. WACCM and GOMOS ozone mixing ratio difference from Fig. 6 in the Arctic 60°N–90°N (blue) and in the Antarctic 60°S–90°S (red).

the correlation is very high 0.85-0.95. At altitudes higher than 1 hPa the correlation declines outside the polar areas, but increases again after the ozone minimum before final decay starting just below the second ozone peak.

Atmos. Chem. Phys. Discuss., https://doi.org/10.5194/acp-2017-1161
Manuscript under review for journal Atmos. Chem. Phys.
Discussion started: 20 December 2017

Atmospheric Chemistry and Physics Discussions

Fig. 5 shows the comparison of the GOMOS and WACCM ozone mixing ratio monthly time series from three latitude bands and at three pressure levels from August 2002 to January 2005. At the second maximum there is a large bias between the WACCM and GOMOS as expected from results already shown. Ozone in all three latitude bands shows semi-annual oscillations. Near the main maximum time series seem to follow each other quite closely and the correlation coefficient is even 0.98. At the lowest altitude we can see that WACCM values in the tropics are consistently higher than GOMOS resulting to the positive tropical bias in Fig. 2 wheres at mid-latitudes there is a good agreement.

In Fig. 6 we show the 5-day ozone mixing ratio time series in both polar regions. The Arctic and Antarctic time series are shown in the same plot because GOMOS nighttime coverage is complementary in these regions. Differences are shown in Fig.7 using the mixing ratio unit. The highest altitude shows again large differences at the second peak. The middle panel shows results near the main ozone peak at the position where Fig. 2 indicated WACCM to be 20% larger than GOMOS in the Arctic. The positive bias seems to be consistent in time and much larger in the north. The lowest altitude shows the regular Antarctic ozone hole pattern. In the Arctic the exceptionally large ozone loss in 2011 (see Manney et al., 2011) is clearly seen.The Antarctic ozone holes are seen equally by WACCM and GOMOS whereas the Arctic hole 2011 is under estimated by WACCM. A similar even larger difference can be seen in 2010 but now without a real large reduction of ozone.

6 Nitrogen dioxide

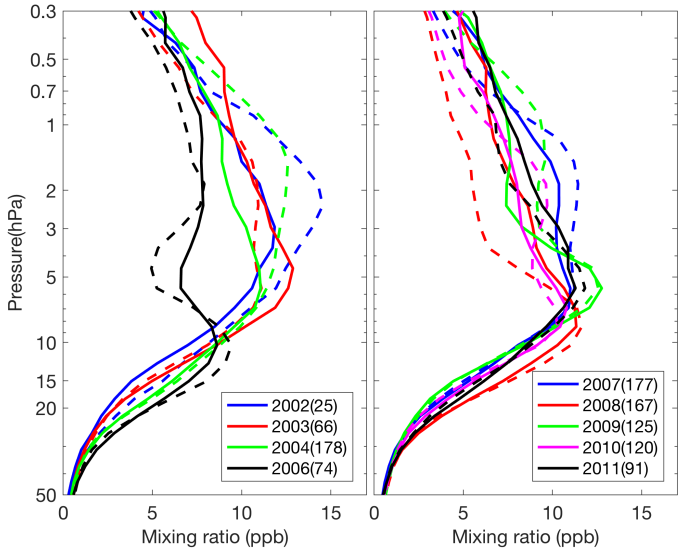

Figure 8. NO_2 yearly median profiles from GOMOS Sirius occultations (solid lines) and paired WACCM profiles (dashed lines) from 2002 to 2011 in the latitude band 40°S–60°S. The colour coding in the legend boxes show the measurement year and in the parenthesis the number of measurements.

Atmos. Chem. Phys. Discuss., https://doi.org/10.5194/acp-2017-1161
Manuscript under review for journal Atmos. Chem. Phys.
Discussion started: 20 December 2017

Atmospheric Chemistry and Physics Discussions

We start again with GOMOS profiles from the Sirius occultations in the latitude band 40°S–60°S in Fig. 8. The validity region for Sirius NO_2 is from 100 hPa to 0.2 hPa in this latitude region. The average uncertainty of the GOMOS and WACCM median profiles is better than 5% in 50–0.5 hPa. The relative GOMOS-WACCM difference is -10–+20% in 50–0.5 hPa. Around the maximum 5 hPa the difference is $\pm$ 3%. The yearly variation in profiles and differences is large.

In Fig. 9 we show the median relative difference between WACCM and GOMOS as a function of latitude and altitude during 2002–2011. The most conspicuous feature of this figure is the variation of the upper valid altitude limit. In the polar regions GOMOS measurements reach up to near 0.05 hPa whereas at the non-polar latitudes the highest altitude is about 0.4 hPa. The lower limit is 72 hPa. The variation of the upper validity limit is the consequence of the data screening using t-values and the positivity condition of the distribution (see Sec. 4). It is important to realise that the high altitude results from the polar regions are solely coming from the few short living NO_2 enhancement events whereas the lower polar altitudes are seen by GOMOS during the whole winter season. In the polar areas at high altitudes WACCM values are lower, by 60%, than GOMOS. High GOMOS NO_2 values are related to extraordinary events that will discussed below. The differences are mostly statistically significant, points where the difference are not significant are marked by crosses. Outside the polar areas the relative difference is 0–10%, near the NO_2 maximum GOMOS and WACCM agree with $\pm$ 5%. The NO_2 maximum is at 1.9 hPa by WACCM and at 2.9 hPa by GOMOS. GOMOS and WACCM NO_2 values agree within the uncertainty estimates of GOMOS data from validation and intercomparison studies except in the polar regions

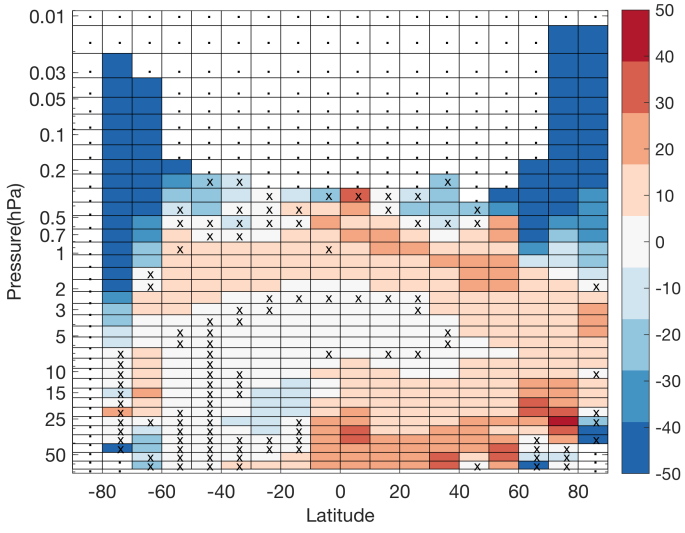

Figure 9. The median relative NO_2 difference (WACCM-GOMOS)/median(GOMOS)) in % over 2002–2011. Latitudes are from -90° to 90° with 10° resolution. A cross marks a point where the difference does not deviate from zero in a statistical significant way. A cell with a dot marks missing data.

Atmos. Chem. Phys. Discuss., https://doi.org/10.5194/acp-2017-1161
Manuscript under review for journal Atmos. Chem. Phys.
Discussion started: 20 December 2017

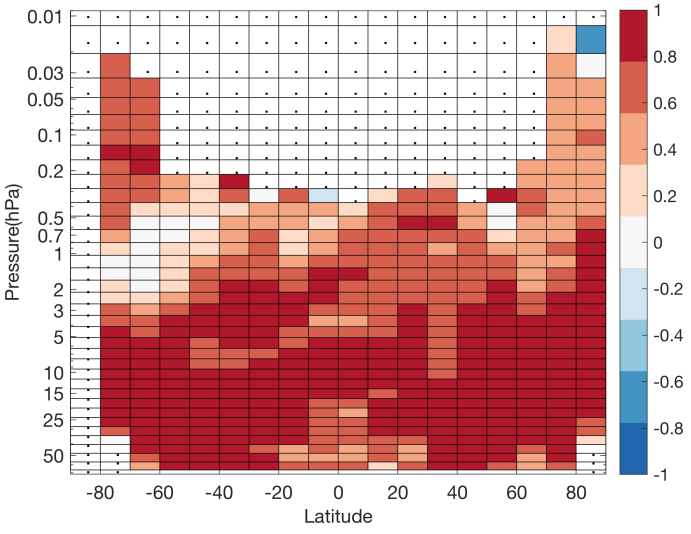

Figure 10. WACCM and GOMOS NO_2 mixing ratio correlation over 2002–2011. Latitudes are from -90° to 90° with 10° resolution. A cell with a dot marks missing data.

Before studying the GOMOS-WACCM disagreement in the polar regions we show in Fig. 10 the GOMOS-WACCM NO_2 correlation coefficient's altitude-latitude distribution. Correlation is relatively high everywhere except in the southern latitudes in the upper stratosphere-lower mesosphere. The moderate correlation in the polar latitudes extends up to the mesosphere even if the mixing ratios differ.

Figure 11 shows GOMOS and WACCM NO_2 time series at three pressure levels in the Arctic and Antarctic from 2002–2011. The differences are shown in Fig. 12 in the mixing ratio unit. In both polar regions almost every winter high NO_2 events are detected at the highest altitude shown. These enhancements are also partly seen at lower altitudes. The most eminent peaks are taking place during the 2003 Antarctic winter and during the Arctic winter 2003–2004. Both events can be distinguished at all three levels shown. We consider in more detail the Arctic event that took place between the end of October 2003 and the end of March 2004. This period covered the strong proton events on October 28–29, 2003 and November 2–3, 2003 (the Halloween event) and the strong descent period that started in mid-January 2004. The complexity of events is illustrated in Fig. 13 and in Fig. 14. From these figures it is clear that mission average results like Fig. 9 cannot be used when we try to find underlying reasons for the differences between GOMOS and WACCM. Various fast processes in the polar regions are so intermingled that investigations must use well resolved time series to separate them.

Elevated NO_2 amounts, observed during the winter periods, are known to be generated by particle precipitation events (see e.g. Seppälä et al., 2004, 2007; Funke et al., 2011) and enhanced downward transport of NO_X from the lower thermosphere (e.g. Hauchecorne et al., 2007; Randall et al., 2009; Päivärinta et al., 2016; Funke et al., 2017). WACCM and GOMOS both capture the enhanced NO_2 values around 0.5 hPa, produced by the SPEs in the end of October, and the descent until mid December.

Atmos. Chem. Phys. Discuss., https://doi.org/10.5194/acp-2017-1161
Manuscript under review for journal Atmos. Chem. Phys.
Discussion started: 20 December 2017

Atmospheric Chemistry and Physics Discussions

WACCM seems to overestimate the magnitude of this enhancement by 5–10 ppb, which is in agreement with earlier results on NO_y (Funke et al., 2011, Fig. 15). WACCM reproduces only a fraction of the larger increase observed at 0.05 hPa in the beginning of December. This is also true for the strong descent from mesosphere to upper stratosphere observed in January–April. Values measured by GOMOS are up to ten times larger than those simulated by WACCM. Mesospheric NO_2, and NO_x in general, have been underestimated in WACCM during this period due to 1) a combination of incomplete simulation of high-energy EEP (i.e., in-situ production) and 2) recovery from a sudden stratospheric warming in early January, resulting in insufficient descent (see (Randall et al., 2015)).

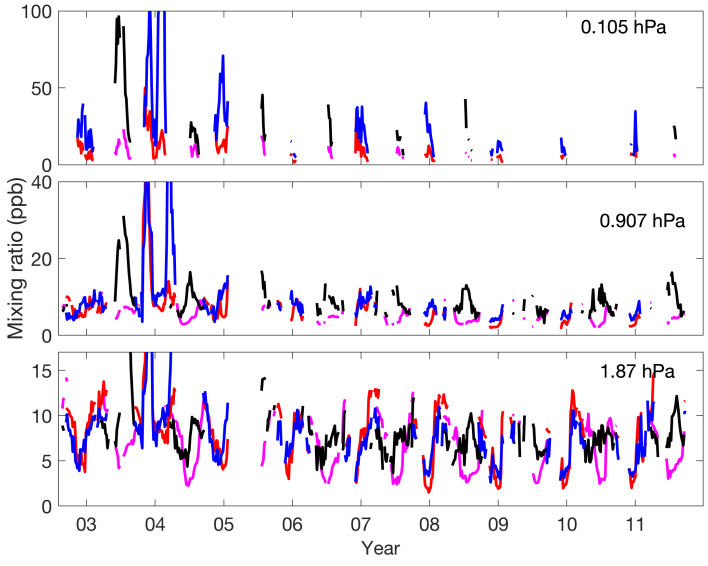

Figure 11. NO_2 mixing ratio 5-day time series at three pressure levels from the Arctic 60°N–90°N (GOMOS: blue, WACCM: red) and the Antarctic 60°S–90°S (GOMOS: black, WACCM: magenta). Notice that the y-axis cuts do not show the full values of NO_2 peaks during November 2003–April 2004. More details from this period are shown in Figs. 13–14.

7 Nitrogen trioxide

In Fig. 15 we show NO_3 profiles from the Sirius occultations in the latitude band 40°S–60°S. The relative uncertainty is better than 10% and the relative difference from -20% to +5% in 1–50 hPa. Near the peak density 2 hPa (40 km) WACCM and GOMOS values are within ± 2% but at lower altitudes WACCM values are consistently about 20% smaller than GOMOS.

In Fig. 16 we show the median relative differences from 2002 to 2011 between GOMOS and WACCM as a function of latitude and altitude. The differences are mostly statistically significant, crossed cells mark differences that are not statistically significant. The GOMOS NO_3 peaks at 1.9 hPa and WACCM at 2.35 hPa. Around the peak of the NO_3 profile the difference between WACCM and GOMOS is inside ±5%. This is much better that uncertainty estimates of GOMOS NO_3. In the polar regions, the maximum region excluded, WACCM NO_3 is up to 60% smaller than GOMOS.

Atmos. Chem. Phys. Discuss., https://doi.org/10.5194/acp-2017-1161
Manuscript under review for journal Atmos. Chem. Phys.
Discussion started: 20 December 2017

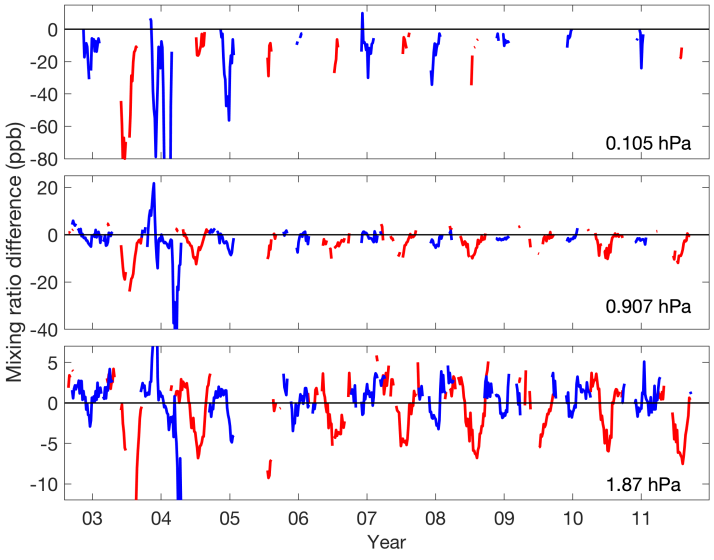

Figure 12. WACCM and GOMOS NO_2 mixing ratio difference 5-day time series 2002–2011 in the Arctic 60°N–90°N (blue) and in the Antarctic 60°S–90°S (red).

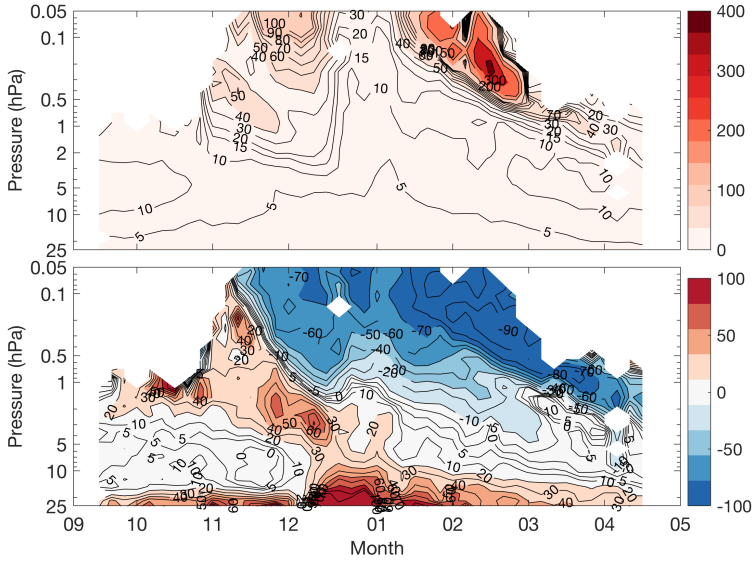

Figure 13. GOMOS NO_2 mixing ratio from 5-day time series (upper panel) and WACCM-GOMOS relative difference (lower panel) from 15.9.2003–31.4.2004 in the Arctic 60°N–90°N.

In Fig. 17 we show the GOMOS-WACCM NO_3 correlation coefficient as a function of the altitude and latitude. Around the NO_3 maximum all latitudes show very high correlations 0.95. The secret behind this high correlation is the fact that the

Atmos. Chem. Phys. Discuss., https://doi.org/10.5194/acp-2017-1161
Manuscript under review for journal Atmos. Chem. Phys.
Discussion started: 20 December 2017

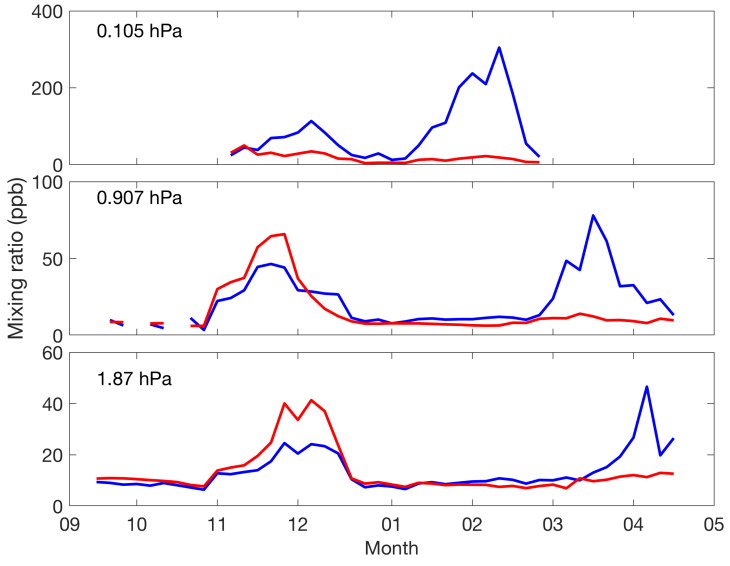

Figure 14. NO_2 mixing ratio at three pressure levels from 5-day time series from GOMOS (blue lines) and WACCM (red lines) from 15.9.2003–31.4.2004 to in the Arctic 60°N–90°N.

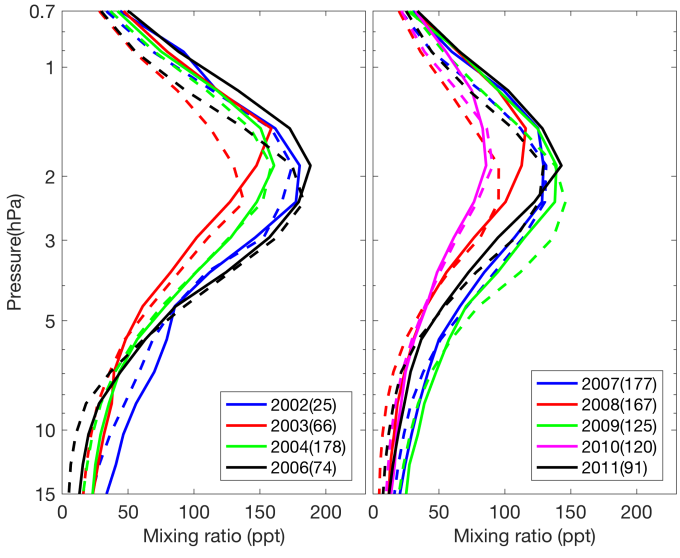

Figure 15. NO_3 median yearly profiles from GOMOS Sirius occultations (solid lines) and paired WACCM profiles(dashed lines) from 2002 to 2011 in the latitude band 40°S–60°S. The colour coding in the legend boxes shows the measurement year and the number of measurements in the parenthesis.

Atmos. Chem. Phys. Discuss., https://doi.org/10.5194/acp-2017-1161
Manuscript under review for journal Atmos. Chem. Phys.
Discussion started: 20 December 2017

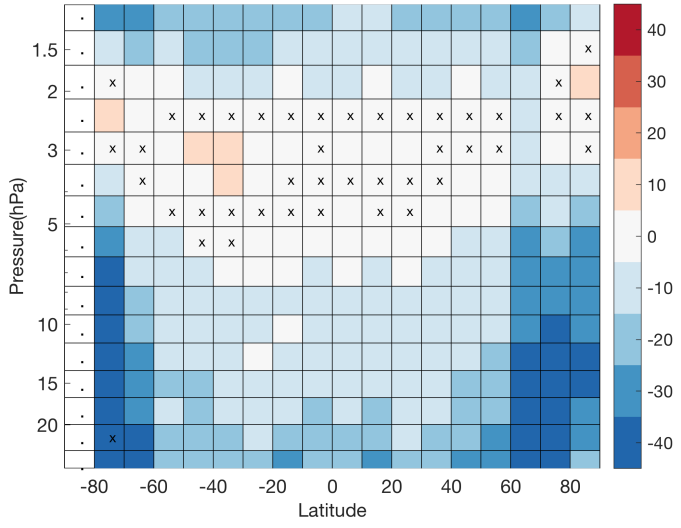

Figure 16. The relative NO_3 difference (WACCM-GOMOS)/median(GOMOS) in % during 2002–2011. Latitudes are from -90° to 90° with 10° resolution. A cross marks a point where the difference does not deviate from zero in a statistical significant way. A cell with a dot marks missing data.

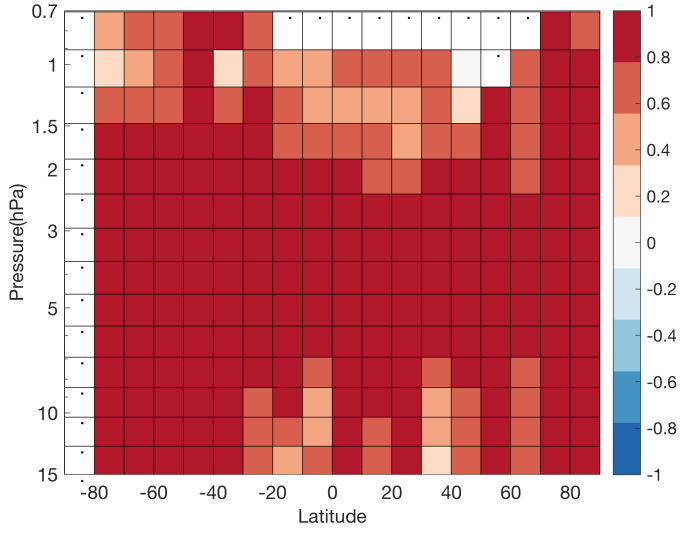

Figure 17. WACCM and GOMOS NO_3 mixing ratio correlation over 2002–2011. Latitudes are from -90° to 90° with 10° resolution. A cell with a dot marks missing data.

Atmos. Chem. Phys. Discuss., https://doi.org/10.5194/acp-2017-1161
Manuscript under review for journal Atmos. Chem. Phys.
Discussion started: 20 December 2017

Atmospheric Chemistry and Physics Discussions

mixing ratio of NO_3 is very sensitive to temperature (see Hauchecorne et al., 2005; Kyrölä et al., 2010a). When we calculate the correlation of WACCM's NO_3 with the model temperature (in the stratosphere MERRA), we get values from 0.8 to 0.95 in the altitude range 2–50 hPa. Between GOMOS NO_3 and MERRA a similar positive correlation is achieved between 2–5 hPa. Temperature-related issues are a probable cause for the observed NO_3 differences in the polar regions evident in Fig. 16. It is plausible to state that in the polar regions MERRA underestimates real temperatures except in the neighbourhood of the NO_3 maximum. The temporal cycle is correct but the absolute values differ.

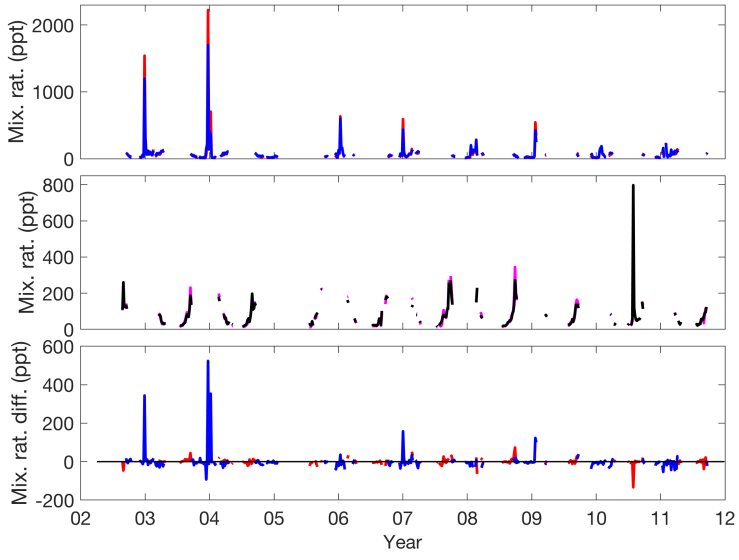

Figure 18. NO_3 mixing ratio 5-day time series at 3.7 hPa from GOMOS (blue lines) and WACCM (red lines) from 2002 to 2011 in the Arctic 60°N–90°N (upper panel) and in the Antarctic 60°S–90°S (middle panel). In the bottom panel the mixing ratio difference is shown for the Arctic (blue) and the Antarctic (red) in the mixing ratio unit.

Dramatic examples about the temperature dependence of NO_3 can be seen in the polar time series of Fig. 18. In the Arctic, the strongest peaks in mixing ratio are caused by the large changes in temperature during Sudden Stratospheric Warming events (e.g. Sofieva et al., 2012; Butler et al., 2017). In the Antarctic the NO_3 cycle follows the normal annual cycle of the temperature with one exception: During the 5-day period around 28 July 2010 NO_3 values have a major jump (for analysis of this case, see de Laat and van Weele (2011)). It seems that at the sudden warmings (with the Antarctic case excluded) WACCM values considerably exceed the corresponding GOMOS values and consequently MERRA overestimates the real temperature. A detailed evolution of the strong Arctic event in December 2003–January 2004 is shown in Fig.19. WACCM and GOMOS values show similar temporal development but the absolute values differ.

We can further study the temperature dependence of NO_3. In Fig. 20 we have plotted GOMOS and WACCM mixing values as a function of MERRA temperature from 3.7 hPa. The dependence on temperature is nearly exponential from both sources in the polar regions. The very high values in the Arctic are not fitted by the exponential function. Tropical values can equally well

Atmos. Chem. Phys. Discuss., https://doi.org/10.5194/acp-2017-1161
Manuscript under review for journal Atmos. Chem. Phys.
Discussion started: 20 December 2017

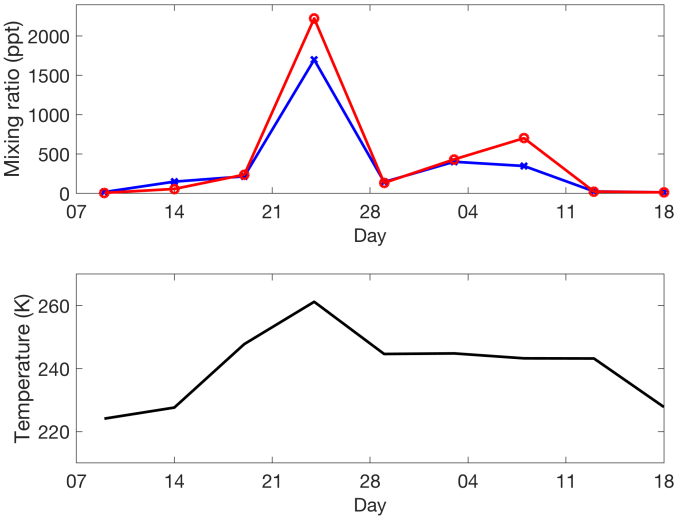

Figure 19. The upper panel: WACCM (red) and GOMOS (blue) NO_3 5-day time series 7.12.2003–18.1.2004 in the Arctic 60°N–90°N at 3.7 hPa. Lower panel: MERRA temperature for the same period and altitude.

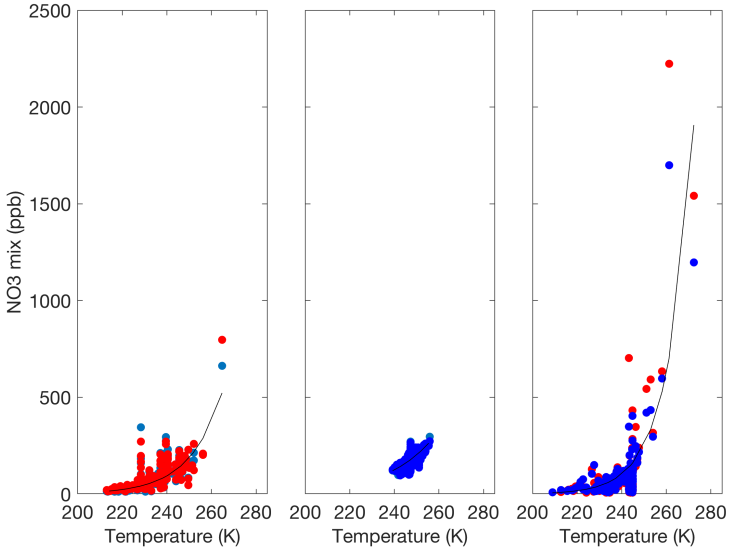

Figure 20. NO_3-temperature scatter-plot at 3.7 hPa. The left panel: the Arctic 60°N–90°N. The middle panel: Tropics 10°S –10°N. The right panel: the Antarctic 60°S –90°S. Red dots are from WACCM and blue dots from GOMOS. Exponential fits are done to temperature gridded WACCM data. Data for all latitudes are from 5-day time series from 2002–2011.

Atmos. Chem. Phys. Discuss., https://doi.org/10.5194/acp-2017-1161
Manuscript under review for journal Atmos. Chem. Phys.
Discussion started: 20 December 2017

Atmospheric Chemistry and Physics Discussions

fitted by a linear model. In ref. Brasseur and Solomon (2005) a formula for the ratio of O_3 to NO_3 densities is derived assuming night time chemical equilibrium. In Fig. 21 we show how the experimental values from GOMOS and modelling values from WACCM compares with this theoretical prediction. The GOMOS-WACCM agreement is very good and the agreement with theory is also good up to 2.1 hPa.

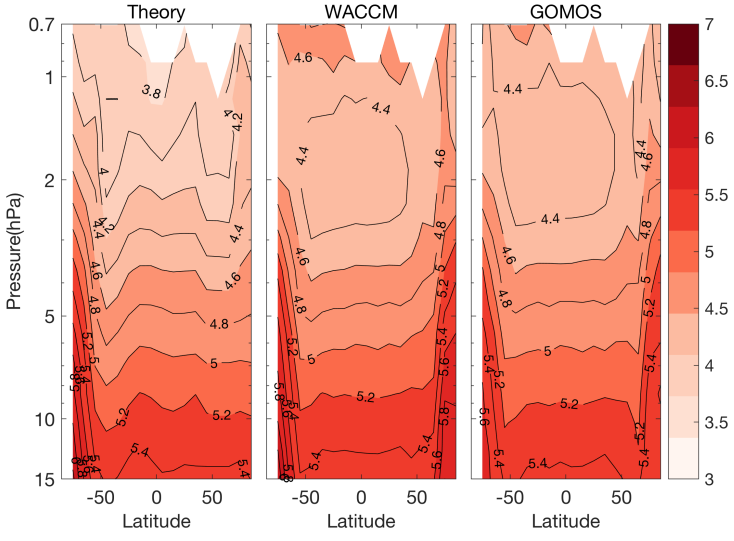

Figure 21. The NO_3/O_3 ratio from the chemical theory in Brasseur and Solomon (2005) (left panel). Ratios calculated from the WACCM simulation (middle panel) and GOMOS measurements (right panel). Data covers 2002–2011.

8 Conclusions

In this work we have compared the state-of-the-art chemistry - climate model WACCM to measurements from the satellite instrument GOMOS. Measurements cover years from 2002 to 2011 and they are from nighttime. We have compared O_3, NO_2 and NO_3 mixing ratios using monthly (non-polar) and 5-day time series. We have also calculated the correlation of GOMOS and WACCM time series. The comparison is done with collocated profiles, which eliminates differences from the natural variability and sampling patterns.

This comparison has required a considerable effort to ensure the quality of the observational data. GOMOS nighttime observations collect photons from 180 different stars varying widely with their luminosity and effective temperature. This variation causes large differences in the quality of trace gas profiles. For ozone we have used three GOMOS ozone data flags to remove hopelessly poor profiles, for NO_2 and NO_3 there are no such quality flags available. The main problem of all GOMOS trace gas profiles is to decide upon the altitude limits of valid data. In the present work we have determined the limits for all the time steps, all latitude bands and for all stars using two criteria. First, we have demanded that for valid altitudes the t-value (GOMOS density/uncertainty) is larger than 2 and second, that the distribution of GOMOS values is located mainly on positive

density values. Moreover, we have rejected orphan valid values. This approach has produced altitude limits of valid data that earlier have been estimated using a priori knowledge.

Our comparisons show that in the stratosphere (50–1 hPa) outside the polar regions differences in ozone between GOMOS and WACCM are small and within the uncertainties of GOMOS measurements. The difference patterns are consistent in time during 2002–2011. In the tropical region in the lower stratosphere WACCM measurements show consistently larger values than GOMOS. In the polar areas GOMOS nighttime measurements show ozone losses that are connected to the elevated NO_2 concentrations from solar storms and strong downdraft events from the thermosphere. In the mesosphere above the ozone minimum at 0.01 hPa (or 80 km) large differences are found between WACCM and GOMOS. Differences exist in the values of the mixing ratio and also in the correlation of monthly time series at the second ozone maximum. Differences may be connected to WACCM's temperatures in the mesosphere or to specific parameter values that control the gravity wave dissipation in WACCM (see Smith et al. (2014)). The correlation of GOMOS and WACCM time series is high except the non-polar region in the mesosphere below the ozone minimum and at the altitudes from the second ozone maximum and above.

Outside the polar areas and in the validity region 50–0.3 hPa WACCM and GOMOS NO_2 values agree reasonably well. In the polar areas, where solar particle precipitation and downward transport from the thermosphere enhance NO_2 abundances, GOMOS values are much larger than WACCM. Correlation of monthly time series is moderate in the stratosphere except the upper stratosphere in the southern latitudes. GOMOS measurements and simulation by the new version of WACCM used in this work agree well for the direct particle initiated NO_2 increases, but for the downdraft cases GOMOS values are much larger. The overall correlation of the polar 5-day time series is still quite high in the middle atmosphere.

For NO_3, we find WACCM values agree largely with GOMOS. In the validity region 25–1.2 hPa the correlation is very high. Because the NO_3 abundance is controlled by temperature the WACCM-GOMOS NO_3 difference can be used as an indicator about the accuracy of MERRA temperature information. We found that NO_3 temperature can be fitted to large extent by an exponential function. The ozone vs. NO_3 ratio follows quite accurately the result from an equilibrium chemical theory. We found that in polar areas the NO_3 mixing ratio can be used as a proxy for Sudden Stratospheric Warmings and provide quality information about the model temperatures.

In this work we have tried to expose agreements and disagreements between the WACCM model and the GOMOS measurements. To understand underlaying reasons for differences a detailed and presumably difficult analysis of the model physics and chemistry. Perhaps the only exception is temperature from the external meteorological model that we think is the reason for NO_3 differences in the polar regions. On the measurement side, there is still room for better algorithms and more extensive validation especially in the polar regions. We have compared O_3, NO_2 and NO_3 distributions between WACCM and GOMOS. A wider comparison including additional constituents from other satellite instruments would help to find the underlaying reasons for differences.

9 Code availability

The SD-WACCM-D model will be available from NCAR. All the WACCM and satellite data have been processed using Matlab-software. The specific routines used in this work can be requested from the first author.

10 Data availability

All data can be requested form the first author. Data will be placed on publicly accessible server in due time. The size of the GOMOS-paired WACCM data set is 2.2 Gb. The GOMOS data used in this work is a Matlab version of the so-called user friendly (UFP) GOMOS data. These UFP data (in netCDF-4 format) are available form the ESA data portal https://earth.esa.int/web/guest/missions/esa-operational-eo-missions/envisat/news/-/article/envisat-gomos-level-2-products-in-netcdf4-change-of-access. The collocated Matlab-data sets include WACCM-data and the paired satellite data. The size: 4.8 Gb.

Competing interests. No competing interests.

Acknowledgements. The work of E.K. was partly supported by ESA's ALGOM-project. The work of M.E.A. and P.T.V. was supported by the Academy of Finland through the project #276926 (SECTIC: Sun-Earth Connection Through Ion Chemistry). D.R.M. was supported in part by NASA grant NNX12AD04G. The National Center for Atmospheric Research is operated by the University Corporation for Atmospheric Research under sponsorship of the National Science Foundation.

References

Andersson, M. E., Verronen, P. T., Marsh, D. R., Päivärinta, S.-M., and Plane, J. M. C.: WACCM-D – Improved modeling of nitric acid and active chlorine during energetic particle precipitation, J. Geophys. Res. (Atmos.), 121, 10,328–10,341, doi:10.1002/2015JD024173, 2016.

Bertaux, J. L., Kyrölä, E., Fussen, D., Hauchecorne, A., Dalaudier, F., Sofieva, V., Tamminen, J., Vanhellemont, F., Fanton D'Andon, O., Barrot, G., Mangin, A., Blanot, L., Lebrun, J. C., Pérot, K., Fehr, T., Saavedra, L., Leppelmeier, G. W., and Fraisse, R.: Global ozone monitoring by occultation of stars: an overview of GOMOS measurements on ENVISAT, Atmospheric Chemistry & Physics, 10, 12 091–12 148, doi:10.5194/acp-10-12091-2010, 2010.

Brasseur, G. P. and Solomon, S.: Aeronomy of the Middle Atmosphere, Springer, Dordrecht, 3rd revised and enlarged edn., 2005.

Butler, A. H., Sjoberg, J. P., Seidel, D. J., and Rosenlof, K. H.: A sudden stratospheric warming compendium, Earth System Science Data, 9, 63–76, doi:10.5194/essd-9-63-2017, 2017.

Ceccherini, S., Cortesi, U., Verronen, P. T., and Kyrölä, E.: Continuity of MIPAS-ENVISAT operational ozone data quality from full- to reduced-spectral-resolution operation mode, Atmos. Chem. Phys., 8, 2201–2212, 2008.

Chandran, A. and Collins, R. L.: Stratospheric sudden warming effects on winds and temperature in the middle atmosphere at middle and low latitudes: a study using WACCM, Annales Geophysicae, 32, 859–874, 2014.

de Laat, A. T. J. and van Weele, M.: The 2010 Antarctic ozone hole: Observed reduction in ozone destruction by minor sudden stratospheric warmings, Scientific Reports, 1, 38, doi:10.1038/srep00038, 2011.

ESA: Envisat-GOMOS, An instrument for global atmospheric ozone monitoring, vol. SP-1244, European Space Agency, Noordwijk, The Netherlands, 2001.

Eyring, V., Shepherd, T. G., and W., W. D., eds.: SPARC CCMVal Report on the Evaluation of Chemistry-Climate Models, vol. No. 5, SPARC Office, http://www.sparc-climate.org/publications/sparc-reports/, 2010.

Eyring, V., Arblaster, J. M., Cionni, I., Sedláček, J., Perlwitz, J., Young, P. J., Bekki, S., Bergmann, D., Cameron-Smith, P., Collins, W. J., Faluvegi, G., Gottschaldt, K. D., Horowitz, L. W., Kinnison, D. E., Lamarque, J. F., Marsh, D. R., Saint-Martin, D., Shindell, D. T., Sudo, K., Szopa, S., and Watanabe, S.: Long-term ozone changes and associated climate impacts in CMIP5 simulations, Journal Of Geophysical Research-Atmospheres, 118, 5029–5060, 2013.

Funke, B., Baumgaertner, A., Calisto, M., Egorova, T., Jackman, C. H., Kieser, J., Krivolutsky, A., López-Puertas, M., Marsh, D. R., Reddmann, T., Rozanov, E., Salmi, S.-M., Sinnhuber, M., Stiller, G. P., Verronen, P. T., Versick, S., von Clarmann, T., Vyushkova, T. Y., Wieters, N., and Wissing, J. M.: Composition changes after the "Halloween" solar proton event: the High-Energy Particle Precipitation in the Atmosphere (HEPPA) model versus MIPAS data intercomparison study, Atmos. Chem. Phys., 11, 9089–9139, doi:10.5194/acp-11-9089-2011, 2011.

Funke, B., Ball, W., Bender, S., Gardini, A., Harvey, V. L., Lambert, A., López-Puertas, M., Marsh, D. R., Meraner, K., Nieder, H., Päivärinta, S.-M., Pérot, K., Randall, C. E., Reddmann, T., Rozanov, E., Schmidt, H., Seppälä, A., Sinnhuber, M., Sukhodolov, T., Stiller, G. P., Tsvetkova, N. D., Verronen, P. T., Versick, S., von Clarmann, T., Walker, K. A., and Yushkov, V.: HEPPA-II model-measurement intercomparison project: EPP indirect effects during the dynamically perturbed NH winter 2008–2009, Atmos. Chem. Phys., 17, 3573–3604, doi:10.5194/acp-17-3573-2017, 2017.

Garcia, R. R., Marsh, D. R., Kinnison, D. E., Boville, B. A., and Sassi, F.: Simulation of secular trends in the middle atmosphere, 1950-2003, Journal of Geophysical Research (Atmospheres), 112, 9301–, doi:10.1029/2006JD007485, 2007.

Hakkarainen, J., Tamminen, J., Moore, J. R., and Kyrölä, E.: Direct comparisons of GOMOS and SAGE III NO_3 vertical profiles, Atmospheric Measurement Techniques, 5, 1841–1846, doi:10.5194/amt-5-1841-2012, 2012.

Hauchecorne, A., Bertaux, J.-L., Dalaudier, F., Cot, C., Lebrun, J.-C., Bekki, S., Marchand, M., Kyrölä, E., Tamminen, J., Sofieva, V., Fussen, D., Vanhellemont, F., Fanton d'Andon, O., Barrot, G., Mangin, A., Théodore, B., Guirlet, M., Snoeij, P., Koopman, R., Saavedra de Miguel, L., Fraisse, R., and Renard, J.-B.: First simultaneous global measurements of nighttime stratospheric NO_2 and NO_3 observed by Global Ozone Monitoring by Occultation of Stars (GOMOS)/Envisat in 2003, J. Geophys. Res., 110, D18 301, doi:10.1029/2004JD005711, 2005.

Hauchecorne, A., Bertaux, J.-L., Dalaudier, F., Russell, J. M., Mlynczak, M. G., Kyrölä, E., and Fussen, D.: Large increase of NO_2 in the north polar mesosphere in January-February 2004: Evidence of a dynamical origin from GOMOS/ENVISAT and SABER/TIMED data, Geophys. Res. Lett., 34, L03 810, doi:10.1029/2006GL027628, 2007.

Hedin, A. E.: Extension of the MSIS thermospheric model into the middle and lower atmosphere, J. Geophys. Res., 96, 1159–1172, 1991.

Hegglin, M. I. and Tegtmeier, S., eds.: The SPARC Data Initiative: Assessment of stratospheric trace gas and aerosol climatologies from satellite limb sounders., vol. No. 8, SPARC Office, http://www.sparc-climate.org/publications/sparc-reports/, 2017.

Hubert, D., Lambert, J.-C., Verhoelst, T., Granville, J., Keppens, A., Baray, J.-L., Bourassa, A. E., Cortesi, U., Degenstein, D. A., Froidevaux, L., Godin-Beekmann, S., Hoppel, K. W., Johnson, B. J., Kyrölä, E., Leblanc, T., Lichtenberg, G., Marchand, M., McElroy, C. T., Murtagh, D., Nakane, H., Portafaix, T., Querel, R., Russell, III, J. M., Salvador, J., Smit, H. G. J., Stebel, K., Steinbrecht, W., Strawbridge, K. B., Stübi, R., Swart, D. P. J., Taha, G., Tarasick, D. W., Thompson, A. M., Urban, J., van Gijsel, J. A. E., Van Malderen, R., von der Gathen, P., Walker, K. A., Wolfram, E., and Zawodny, J. M.: Ground-based assessment of the bias and long-term stability of 14 limb and occultation ozone profile data records, Atmospheric Measurement Techniques, 9, 2497–2534, doi:10.5194/amt-9-2497-2016, 2016.

Jackman, C. H., Marsh, D. R., Vitt, F. M., Roble, R. G., Randall, C. E., Bernath, P. F., Funke, B., López-Puertas, M., Versick, S., Stiller, G. P., Tylka, A. J., and Fleming, E. L.: Northern Hemisphere atmospheric influence of the solar proton events and ground level enhancement in January 2005, Atmos. Chem. Phys., 11, 6153–6166, doi:10.5194/acp-11-6153-2011, 2011.

Jackman, C. H., Marsh, D. R., Kinnison, D. E., Mertens, C. J., and Fleming, E. L.: Atmospheric changes caused by galactic cosmic rays over the period 1960–2010, Atmos. Chem. Phys., 16, 5853–5866, doi:10.5194/acp-16-5853-2016, 2016.

Kerzenmacher, T., Wolff, M. A., Strong, K., Dupuy, E., Walker, K. A., Amekudzi, L. K., Batchelor, R. L., Bernath, P. F., Berthet, G., Blumenstock, T., Boone, C. D., Bramstedt, K., Brogniez, C., Brohede, S., Burrows, J. P., Catoire, V., Dodion, J., Drummond, J. R., Dufour, D. G., Funke, B., Fussen, D., Goutail, F., Griffith, D. W. T., Haley, C. S., Hendrick, F., Höpfner, M., Huret, N., Jones, N., Kar, J., Kramer, I., Llewellyn, E. J., López-Puertas, M., Manney, G., McElroy, C. T., McLinden, C. A., Melo, S., Mikuteit, S., Murtagh, D., Nichitiu, F., Notholt, J., Nowlan, C., Piccolo, C., Pommereau, J., Randall, C., Raspollini, P., Ridolfi, M., Richter, A., Schneider, M., Schrems, O., Silicani, M., Stiller, G. P., Taylor, J., Tétard, C., Toohey, M., Vanhellemont, F., Warneke, T., Zawodny, J. M., and Zou, J.: Validation of NO_2 and NO from the Atmospheric Chemistry Experiment (ACE), Atmos. Chem. Phys., 8, 5801–5841, 2008.

Kyrölä, E., Tamminen, J., Sofieva, V., Bertaux, J. L., Hauchecorne, A., Dalaudier, F., Fussen, D., Vanhellemont, F., Fanton D'Andon, O., Barrot, G., Guirlet, M., Fehr, T., and Saavedra de Miguel, L.: GOMOS O_3, NO_2, and NO_3 observations in 2002-2008, Atmospheric Chemistry and Physics, 10, 7723–7738, doi:10.5194/acp-10-7723-2010, http://www.atmos-chem-phys.net/10/7723/2010/, 2010a.

Kyrölä, E., Tamminen, J., Sofieva, V., Bertaux, J. L., Hauchecorne, A., Dalaudier, F., Fussen, D., Vanhellemont, F., Fanton D'Andon, O., Barrot, G., Guirlet, M., Mangin, A., Blanot, L., Fehr, T., Saavedra de Miguel, L., and Fraisse, R.: Retrieval of atmospheric parameters from GOMOS data, Atmospheric Chemistry & Physics, 10, 11 881–11 903, doi:10.5194/acp-10-11881-2010, 2010b.

Kyrölä, E., Laine, M., Sofieva, V., Tamminen, J., Päivärinta, S.-M., Tukiainen, S., Zawodny, J., and Thomason, L.: Combined SAGE II -GOMOS ozone profile data set for 1984–2011 and trend analysis of the vertical distribution of ozone, Atmospheric Chemistry and Physics, 13, 10 645–10 658, doi:10.5194/acp-13-10645-2013, http://www.atmos-chem-phys.net/13/10645/2013/, 2013.

Lary, D. J.: Catalytic destruction of stratospheric ozone, J. Geophys. Res., 102, 21 515–21 526, doi:10.1029/97JD00912, 1997.

Lean, J., Rottman, G., Harder, J., and Kopp, G.: SORCE Contributions to New Understanding of Global Change and Solar Variability, Solar Physics, 230, 27–53, doi:10.1007/s11207-005-1527-2, 2005.

Manney, G. L., Santee, M. L., Rex, M., Livesey, N. J., Pitts, M. C., Veefkind, P., Nash, E. R., Wohltmann, I., Lehmann, R., Froidevaux, L., Poole, L. R., Schoeberl, M. R., Haffner, D. P., Davies, J., Dorokhov, V., Gernandt, H., Johnson, B., Kivi, R., Kyrö, E., Larsen, N., Levelt, P. F., Makshtas, A., McElroy, C. T., Nakajima, H., Parrondo, M. C., Tarasick, D. W., von der Gathen, P., Walker, K. A., and Zinoviev, N. S.: Unprecedented Arctic ozone loss in 2011, Nature, 478, 469–475, 2011.

Marsh, D., Smith, A., Brasseur, G., Kaufmann, M., and Grossmann, K.: The existence of a tertiary ozone maximum in the high latitude middle mesosphere, Geophys. Res. Lett., 28, 4531–4534, 2001.

Marsh, D. R., Mills, M., Kinnison, D., Lamarque, J.-F., Calvo, N., and Polvani, L.: Climate change from 1850 to 2005 simulated in CESM1(WACCM), J. Climate, 26, 7372–7391, doi:10.1175/JCLI-D-12-00558, 2013.

Matthes, K., Funke, B., Andersson, M. E., Barnard, L., Beer, J., Charbonneau, P., Clilverd, M. A., Dudok de Wit, T., Haberreiter, M., Hendry, A., Jackman, C. H., Kretschmar, M., Kruschke, T., Kunze, M., Langematz, U., Marsh, D. R., Maycock, A., Misios, S., Rodger, C. J., Scaife, A. A., Seppälä, A., Shangguan, M., Sinnhuber, M., Tourpali, K., Usoskin, I., van de Kamp, M., Verronen, P. T., and Versick, S.: Solar Forcing for CMIP6, Geosci. Model Dev., 10, 2247–2302, doi:10.5194/gmd-10-2247-2017, 2016.

Meijer, Y. J., Swart, D. P. J., Allaart, M., Andersen, S. B., Bodeker, G., Boyd, I., Braathen, G., Calisesi, Y., Claude, H., Dorokhov, V., von der Gathen, P., Gil, M., Godin-Beekmann, S., Goutail, F., Hansen, G., Karpetchko, A., Keckhut, P., Kelder, H. M., Koelemeijer, R., Kois, B., Koopman, R. M., Kopp, G., Lambert, J.-C., Leblanc, T., McDermid, I. S., Pal, S., Schets, H., Stubi, R., Suortti, T., Visconti, G., and Yela, M.: Pole-to-pole validation of Envisat GOMOS ozone profiles using data from ground-based and balloon sonde measurements, Journal of Geophysical Research (Atmospheres), 109, D23305, doi:10.1029/2004JD004834, 2004.

Morgenstern, O., Hegglin, M. I., Rozanov, E., O amp apos Connor, F. M., Abraham, N. L., Akiyoshi, H., Archibald, A. T., Bekki, S., Butchart, N., Chipperfield, M. P., Deushi, M., Dhomse, S. S., Garcia, R. R., Hardiman, S. C., Horowitz, L. W., Jöckel, P., Josse, B., Kinnison, D., Lin, M., Mancini, E., Manyin, M. E., Marchand, M., Marécal, V., Michou, M., Oman, L. D., Pitari, G., Plummer, D. A., Revell, L. E., Saint-Martin, D., Schofield, R., Stenke, A., Stone, K., Sudo, K., Tanaka, T. Y., Tilmes, S., Yamashita, Y., Yoshida, K., and Zeng, G.: Review of the global models used within phase 1 of the Chemistry–Climate Model Initiative (CCMI), Geoscientific Model Development, 10, 639–671, 2017.

Neale, R. B., Richter, J., Park, S., Lauritzen, P. H., Vavrus, S. J., Rasch, P. J., and Zhang, M.: The Mean Climate of the Community Atmosphere Model (CAM4) in Forced SST and Fully Coupled Experiments, Journal of Climate, 26, 5150–5168, doi:10.1175/JCLI-D-12-00236.1, 2013.

Päivärinta, S.-M., Verronen, P. T., Funke, B., Gardini, A., Seppälä, A., and Andersson, M. E.: Transport versus energetic particle precipitation: Northern polar stratospheric NO_x and ozone in January-March 2012, J. Geophys. Res. (Atmos.), 121, 6085–6100, doi:10.1002/2015JD024217, 2016.

Randall, C. E., Harvey, V. L., Siskind, D. E., France, J., Bernath, P. F., Boone, C. D., and Walker, K. A.: NO_x descent in the Arctic middle atmosphere in early 2009, Geophys. Res. Lett., 36, L18 811, doi:10.1029/2009GL039706, 2009.

Randall, C. E., Harvey, V. L., Holt, L. A., Marsh, D. R., Kinnison, D., Funke, B., and Bernath, P. F.: Simulation of energetic particle precipitation effects during the 2003–2004 Arctic winter, J. Geophys. Res. (Space Phys.), 120, 5035–5048, doi:10.1002/2015JA021196, 2015.

Renard, J., Berthet, G., Brogniez, C., Catoire, V., Fussen, D., Goutail, F., Oelhaf, H., Pommereau, J., Roscoe, H. K., Wetzel, G., Chartier, M., Robert, C., Balois, J., Verwaerde, C., Auriol, F., François, P., Gaubicher, B., and Wursteisen, P.: Validation of GOMOS-Envisat vertical profiles of O_3, NO_2, NO_3, and aerosol extinction using balloon-borne instruments and analysis of the retrievals, Journal of Geophysical Research (Space Physics), 113, A02 302, doi:10.1029/2007JA012345, 2008.

Rienecker, M. M., Suarez, M. J., Gelaro, R., Todling, R., Bacmeister, J., Liu, E., Bosilovich, M. G., Schubert, S. D., Takacs, L., Kim, G.-K., Bloom, S., Chen, J., Collins, D., Conaty, A., da Silva, A., Gu, W., Joiner, J., Koster, R. D., Lucchesi, R., Molod, A., Owens, T., Pawson, S., Pegion, P., Redder, C. R., Reichle, R., Robertson, F. R., Ruddick, A. G., Sienkiewicz, M., and Woollen, J.: MERRA: NASA's Modern-Era Retrospective Analysis for Research and Applications, Journal of Climate, 24, 3624–3648, doi:10.1175/JCLI-D-11-00015.1, 2011.

Sakazaki, T., Shiotani, M., Suzuki, M., Kinnison, D., Zawodny, J. M., McHugh, M., and Walker, K. A.: Sunset–sunrise difference in solar occultation ozone measurements (SAGE II, HALOE, and ACE–FTS) and its relationship to tidal vertical winds, Atmospheric Chemistry And Physics, 15, 829–843, 2015.

Schmidt, H., Brasseur, G. P., Charron, M., Manzini, E., Giorgetta, M. A., Diehl, T., Fomichev, V. I., Kinnison, D., Marsh, D., and Walters, S.: The HAMMONIA chemistry climate model: Sensitivity of the mesopause region to the 11-year solar cycle and CO2 doubling, J. Climate, 19, 3903–3931, 2006.

Seppälä, A., Verronen, P. T., Kyrölä, E., Hassinen, S., Backman, L., Hauchecorne, A., Bertaux, J. L., and Fussen, D.: Solar proton events of October-November 2003: Ozone depletion in the Northern Hemisphere polar winter as seen by GOMOS/Envisat, Geophys. Res. Lett., 31, L19 107, doi:10.1029/2004GL021042, 2004.

Seppälä, A., Verronen, P. T., Clilverd, M. A., Randall, C. E., Tamminen, J., Sofieva, V. F., Backman, L., and Kyrölä, E.: Arctic and Antarctic polar winter NO_x and energetic particle precipitation in 2002–2006, Geophys. Res. Lett., 34, L12 810, doi:10.1029/2007GL029733, 2007.

Smith, A. K., Marsh, D. R., Russell, J. M., Mlynczak, M. G., Martin-Torres, F. J., and Kyrölä, E.: Satellite observations of high nighttime ozone at the equatorial mesopause, Journal of Geophysical Research (Atmospheres), 113, D17 312, doi:10.1029/2008JD010066, 2008.

Smith, A. K., López-Puertas, M., García-Comas, M., and Tukiainen, S.: SABER observations of mesospheric ozone during NH late winter 2002–2009, Geophys. Res. Lett., 36, L23 804, doi:10.1029/2009GL040942, 2009.

Smith, A. K., Rolando, R. R., Marsh, D. R., and Richter, J. H.: WACCM simulations of the mean circulation and trace species transport in the winter mesosphere, J. Geophys. Res., 116, D20 115, doi:10.1029/2011JD016083, 2011.

Smith, A. K., Harvey, V. L., Mlynczak, M. G., Funke, B., GarcíA-Comas, M., Hervig, M., Kaufmann, M., KyröLä, E., López-Puertas, M., McDade, I., Randall, C. E., Russell, J. M., Sheese, P. E., Shiotani, M., Skinner, W. R., Suzuki, M., and Walker, K. A.: Satellite observations of ozone in the upper mesosphere, Journal of Geophysical Research (Atmospheres), 118, 5803–5821, doi:10.1002/jgrd.50445, 2013.

Smith, A. K., Lopez-Puertas, M., Funke, B., Garcia-Comas, M., Mlynczak, M. G., and Holt, L. A.: Nighttime ozone variability in the high latitude winter mesosphere, Journal of Geophysical Research (Atmospheres), 119, 13, doi:10.1002/2014JD021987, 2014.

Sofieva, V. F., Kyrölä, E., Verronen, P. T., Seppälä, A., Tamminen, J., Marsh, D. R., Smith, A. K., Bertaux, J.-L., Hauchecorne, A., Dalaudier, F., Fussen, D., Vanhellemont, F., Fanton d'Andon, O., Barrot, G., Guirlet, M., Fehr, T., and Saavedra, L.: Spatio-temporal observations of the tertiary ozone maximum, Atmos. Chem. Phys., 9, 4439–4445, doi:10.5194/acp-9-4439-2009, http://www.atmos-chem-phys.net/9/4439/2009/, 2009.

Sofieva, V. F., Kalakoski, N., Verronen, P. T., Päivärinta, S.-M., Kyrölä, E., Backman, L., and Tamminen, J.: Polar-night O_3, NO_2 and NO_3 distributions during sudden stratospheric warmings in 2003-2008 as seen by GOMOS/Envisat, Atmos. Chem. Phys., 12, 1051–1066, doi:10.5194/acp-12-1051-2012, 2012.

Sofieva, V. F., Ialongo, I., Hakkarainen, J., Kyrölä, E., Tamminen, J., Laine, M., Hauchecorne, A., Dalaudier, F., Bertaux, J.-L., Fussen, D., Blanot, L., Barrot, G., and Dehn, A.: Improved GOMOS/Envisat ozone retrievals in the upper troposphere and the lower stratosphere, Atmospheric Measurement Techniques Discussions, 2016, 1–26, doi:10.5194/amt-2016-219, http://www.atmos-meas-tech-discuss.net/amt-2016-219/, 2016.

Tamminen, J., Kyrölä, E., Sofieva, V. F., Laine, M., Bertaux, J., Hauchecorne, A., Dalaudier, F., Fussen, D., Vanhellemont, F., Fanton-D'Andon, O., Barrot, G., Mangin, A., Guirlet, M., Blanot, L., Fehr, T., Saavedra de Miguel, L., and Fraisse, R.: GOMOS data characterisation and error estimation, Atmospheric Chemistry & Physics, 10, 9505–9519, doi:10.5194/acp-10-9505-2010, 2010.

Tegtmeier, S., Hegglin, M. I., Anderson, J., Bourassa, A., Brohede, S., Degenstein, D., Froidevaux, L., Fuller, R., Funke, B., Gille, J., Jones, A., Kasai, Y., Krüger, K., Kyrölä, E., Lingenfelser, G., Lumpe, J., Nardi, B., Neu, J., Pendlebury, D., Remsberg, E., Rozanov, A., Smith, L., Toohey, M., Urban, J., Clarmann, T., Walker, K. A., and Wang, R. H. J.: SPARC Data Initiative: A comparison of ozone climatologies from international satellite limb sounders, Journal of Geophysical Research (Atmospheres), 118, 12 229, doi:10.1002/2013JD019877, 2013.

Tilmes, S., Lamarque, J.-F., Emmons, L. K., Kinnison, D. E., Marsh, D., Garcia, R. R., Smith, A. K., Neely, R. R., Conley, A., Vitt, F., Val Martin, M., Tanimoto, H., Simpson, I., Blake, D. R., and Blake, N.: Representation of the Community Earth System Model (CESM1) CAM4-chem within the Chemistry-Climate Model Initiative (CCMI), Geoscientific Model Development, 9, 1853–1890, 2016.

Tweedy, O. V., Limpasuvan, V., Orsolini, Y. J., Smith, A. K., Garcia, R. R., Kinnison, D., Randall, C. E., Kvissel, O.-K., Stordal, F., Harvey, V. L., and Chandran, A.: Nighttime secondary ozone layer during major stratospheric sudden warmings in specified-dynamics WACCM, Journal of Geophysical Research (Atmospheres), 118, 8346–8358, doi:10.1002/jgrd.50651, 2013.

van de Kamp, M., Seppälä, A., Clilverd, M. A., Rodger, C. J., Verronen, P. T., and Whittaker, I. C.: A model providing long-term datasets of energetic electron precipitation during geomagnetic storms, J. Geophys. Res. (Atmos.), 121, 12 520–12 540, doi:10.1002/2015JD024212, 2016.

van Gijsel, J. A. E., Swart, D. P. J., Baray, J., Bencherif, H., Claude, H., Fehr, T., Godin-Beekmann, S., Hansen, G. H., Keckhut, P., Leblanc, T., McDermid, I. S., Meijer, Y. J., Nakane, H., Quel, E. J., Stebel, K., Steinbrecht, W., Strawbridge, K. B., Tatarov, B. I., and Wolfram, E. A.: GOMOS ozone profile validation using ground-based and balloon sonde measurements, Atmospheric Chemistry & Physics, 10, 10 473–10 488, 2010.

Verronen, P. T., Kyrölä, E., Tamminen, J., Funke, B., Gil-López, S., Kaufmann, M., López-Puertas, M., von Clarmann, T., Stiller, G., Grabowski, U., and Höpfner, M.: A comparison of night-time GOMOS and MIPAS ozone profiles in the stratosphere and mesosphere, Adv. Space Res., 36, 958–966, 2005.

Verronen, P. T., Ceccherini, S., Cortesi, U., Kyrölä, E., and Tamminen, J.: Statistical comparison of night-time NO_2 observations in 2003–2006 from GOMOS and MIPAS instruments, Adv. Space Res., 43, 1918–1925, doi:10.1016/j.asr.2009.01.027, 2009.

Verronen, P. T., Andersson, M. E., Marsh, D. R., Kovács, T., and Plane, J. M. C.: WACCM-D – Whole Atmosphere Community Climate Model with D-region ion chemistry, J. Adv. Model. Earth Syst., 8, 954–975, doi:10.1002/2015MS000592, 2016.